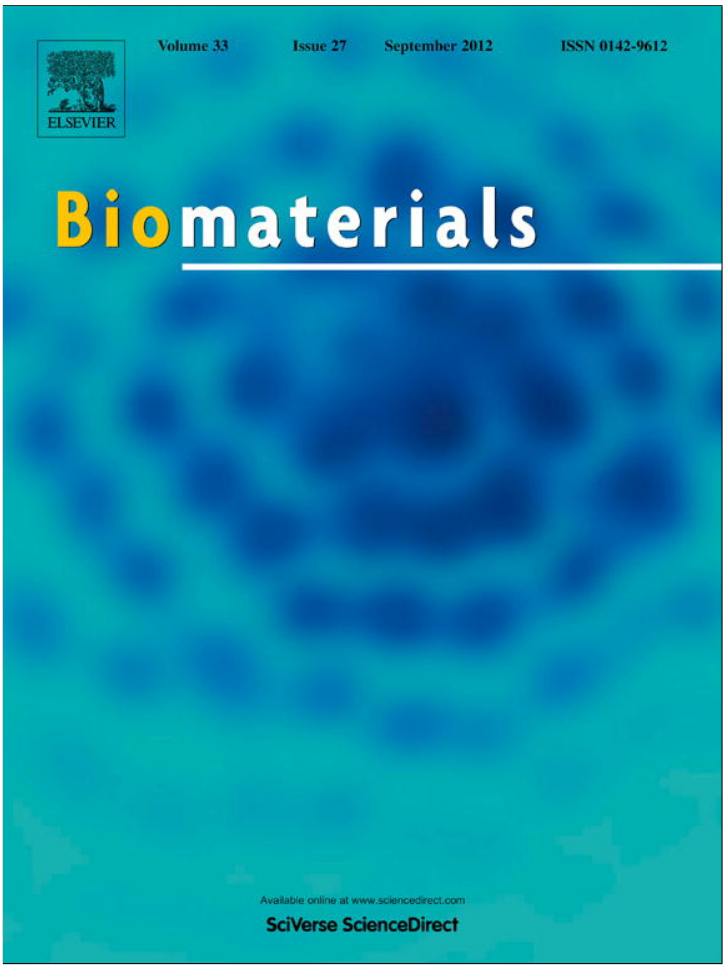

Biomaterials 33 (2012) 6430–6437

Contents lists available at SciVerse ScienceDirect

Biomaterials

journal homepage: www.elsevier.com/locate/biomaterials

Dual optical biosensors for imaging microRNA-1 during myogenesis

Won Jun Kang [a], Ye Lim Cho [a], Ju Ri Chae [a], Jong Doo Lee [a], Bahy A. Ali [b,d], Abdulaziz A. Al-Khedhairy [b], Chang Hyun Lee [c], Soonhag Kim [c,*]

[a] Division of Nuclear Medicine, Department of Radiology, Yonsei University College of Medicine, South Korea
[b] Department of Zoology, College of Science, King Saud University, Riyadh, Saudi Arabia
[c] Laboratory of Molecular Imaging, Department of Biomedical Science, CHA University, South Korea
[d] Department of Nucleic Acids Research, Genetic Engineering and Biotechnology Research Institute, City for Scientific Research and Technology Applications, Alexandria, Egypt

ARTICLE INFO

Article history:
Received 17 May 2012
Accepted 23 May 2012
Available online 12 June 2012

Keywords:
Biosensor
microRNA-1
Molecular beacon
Reporter gene
Myogenic differentiation
Molecular imaging

ABSTRACT

Dual optical microRNA (miRNA) imaging systems, bioluminescent reporter gene (a signal-off mechanism)- or fluorescent molecular beacon (MB) (a signal-on mechanism)-based miRNA imaging system, have individually allowed us to sense miRNA biogenesis in a noninvasive and iterative manner. Both of these imaging systems have shortcomings with respect to image quality. Therefore, we designed a dual optical imaging systems by simultaneous imaging of a miRNA-1 reporter gene (CMV/Gluc/3xPT_miR-1) and miRNA-1 MB in a single cell to overcome these limitations and used it to visualize miRNA-1, a highly expressed miRNA in cardiac and skeletal muscle. During myogenic differentiation of C2C12 cells, the bioluminescence intensity from CMV/Gluc/3xPT_miR-1 revealed a miRNA-1-dependent gradual decrease and the fluorescence intensity from miR-1 MB demonstrated a miRNA-1-dependent gradual increase both *in vitro* and *in vivo*. The dual miRNA-1 imaging systems, which provides the complementary imaging information about miRNA biogenesis, could be useful to sense miRNA expression during various biologic processes.

1. Introduction

MicroRNAs (miRNA, miR) are small non-coding RNAs that regulate gene expression post-transcriptionally [1,2]. MiRNAs are associated with multiple cellular processes including development, differentiation, proliferation, apoptosis, and disease progression [3–7]. MiRNAs are expressed in a tissue-specific manner, and several miRNAs including miRNA-1, miRNA-133, miRNA-181, miRNA-206, and miRNA-26a have been reported to be associated with cardiac and skeletal muscular proliferation and differentiation [8–14]. Of them, miRNA-1 is expressed specifically in skeletal and cardiac muscle, and increasing expression of miRNA-1 has been found in the developing heart [14–17].

The expression of specific miRNAs can be assessed using various methods including microarray, Northern blot and real-time polymerase chain reaction (PCR) [18–23]. However, dynamic changes in miRNA expression in the same subject during cellular processes can not be fully and repeatedly evaluated using these methods. Molecular imaging can be an appropriate method for monitoring miRNA expression during specific cellular processes in a noninvasive and iterative manner. Recently, we have developed two kinds of molecular imaging systems to visualize miRNA expression *in vitro* and *in vivo*. One consists of a bioluminescent miRNA reporter gene system that has binding sequences hybridized to a target miRNA in the 3′ untranslated regions (UTRs) of Gaussia luciferase (Gluc) [24–29]. Although this bioluminescence imaging system is good for *in vivo* imaging of miRNA due to the high signal to background ratio, it functions as a signal-off system because base pairing between binding sequences in the 3′ UTR of the reporter gene and the target miRNA inhibit Gluc expression. Such a signal-off system may be unable to differentiate between decreased Gluc signals resulting from increased miRNA expression and cellular death. The companion imaging system is a fluorescent signal-on imaging system using a MB-based miRNA imaging probe [30,31]. The miRNA MB is a stem-loop-structured DNA oligonucleotide with a fluorescent probe and a quenching molecule at each end with complementary binding sequences to a target miRNA located between them. The stem-loop structure in the miRNA MB is preserved in the absence of a target miRNA, resulting in a quenched fluorescence state by fluorescence resonance energy transfer (FRET) between a fluorescent probe and quenching molecule. In the presence of a target miRNA, binding to the miRNA MB allows

* Corresponding author. Laboratory of Molecular Imaging, Department of Applied Bioscience, CHA University, 605-21, Yeoksam1-dong, Gangnam-gu, Seoul 130-081, South Korea. Tel.: +82 2 555 5063; fax: +82 2 3668 7090.
E-mail address: kimsoonhag@empal.com (S. Kim).

0142-9612/$ – see front matter © 2012 Elsevier Ltd. All rights reserved.
doi:10.1016/j.biomaterials.2012.05.056

substantial distance between the fluorescent probe and quenching molecule, causing recovery of fluorescence. Therefore, the fluorescence signals of the miRNA MB imaging system are increased in proportion to increased target miRNA. Although the miRNA MB is a convenient signal-on imaging system, it is still difficult to obtain high quality *in vivo* images due to a high autofluorescence background caused by external light sources.

A molecular imaging system consisting of both a reporter gene and a MB to monitor miRNA *in vitro* and *in vivo* has advantages and disadvantages. To overcome the shortcomings of each individual miRNA imaging system by providing complementary information, a dual optical miRNA imaging systems consisting of both reporter gene-based signal-off and MB-based signal-on imaging probes was used to monitor the muscle-specific miRNA-1. Using the dual optical miRNA-1 imaging systems, bioluminescence and fluorescence imaging modalities could successfully and simultaneously visualize miRNA-1 biogenesis in a single C2C12 cell (a mouse myoblast cell line) during myogenesis by the miRNA-1 reporter gene and the miR-1 MB *in vitro* and *in vivo*.

2. Materials and methods

2.1. Cell culture

C2C12 and HeLa cells were purchased from the American Type Culture Collection (ATCC). The culture medium for C2C12 and HeLa cells consisted of Dulbecco's modified Eagle's medium (DMEM) and 10% fetal bovine serum (FBS). Medium was changed to DMEM with 1% FBS for induction of differentiation.

2.2. Quantification of miRNA-1 expression

Expression of miRNA-1 from C2C12, HT-ori3, ARO, H9C2 (ATCC; CRL-1446), C6 (ATCC; CCL-107), and HeLa cells were quantified by real-time reverse transcription (RT)-PCR using total RNA. HT-ori3 and ARO cells were kindly provided by Dr. Dongsoo Lee in Seoul National University. Real-time PCR of mature miR-1 was conducted using the mirVanaTM qRT-PCR primer Set and the mirVanaTM qRT-PCR miRNA kit (both from Ambion). PCRs were performed in triplicate using an iCycer (Bio-Rad, USA) and SYBR Premix Ex Taq™ (2×; Takara, Japan) at 95 °C for 3 min and 40 cycles of 95 °C for 15 s and 60 °C for 30 s. The relative amounts of each mature miRNA were normalized versus the U6 snRNA primer set (Ambion) using the equation $2-\Delta\Delta CT$, where $\Delta CT = (CTmiRNA-CTU6RNA)$, $\Delta\Delta CT = (\Delta CT-\Delta CTmiRNA$ of HT-ori3). Data were expressed as mean and standard deviation of realtive values obtained from three different samples. *T*-test was performed with significant *p*-value of 0.05 for comparison.

2.3. Design of miRNA-1 molecular beacon

Mouse miRNA-1 was purchased from Bionics (Bionics, Seoul, Korea). The sequence of miRNA-1 was as follows: 5′TGGAATGTAAAGAAGTATGTAT3′. MB having reverse complimentary sequences to miRNA-1 were synthesized. MiR-1 MB was designed to have Texas Red-X (absorbance/emission wavelength: 590/615 nm) as a fluorophore and BHQ2 as a quencher. The sequences of miRNA-1 molecular beacon was as follows: Texas Red-5′ TGGAAATACATACTTCTTTACATTCCA 3′-BHQ2. As a control, miRNA-9 was purchased from Bionics. The sequence of miRNA-9 was as follows: 5′ UAAAGCUAGAUAACCGAAAGU 3′.

2.4. Fluorescence intensity of molecular beacon

HeLa cells (ATCC) were seeded into 24-well plates at 2×10^4 cells per well. After 24 h, cells were transfected with 50 pmole of miR-1 MB using LipofectAMINE Plus reagent (Invitrogen). Fluorescence intensity was measured from day 0 to day 6 to confirm stability of the MB in HeLa cells.

To validate the correlation of miRNA-1 and the miR-1 MB, target miRNA-1 was applied to each well containing miR-1 MB (50 pmol)-transfected HeLa cells at concentrations of 0, 0.01, 0.025, 0.05, 0.1, 0.5, 0.75, and 1 nM. One nanomole of target miRNA-9 was used as a negative control. After incubation for 3 h at 37 °C, fluorescence intensity was measured at absorbance/emission wavelength with 590/615 nm (Varioskan Flash, Thermo Scientific Co.). C2C12 cells were seeded into 24-well plates at 2×10^4 cells per well. After 24 h, 50 pmole of miR-1 MB was transfected into the C2C12 cells. The transfection procedure was the same as for the HeLa cells. After incubation for 3 h at 37 °C, growth medium was replaced by differentiation medium (DMEM, 1% FBS) to induce myogenic differentiation. On differentiation days 0, 2, 4, and 6, fluorescence intensity was measured to visualize MB activity responding to intrinsic miRNA-1 expression (Varioskan Flash, Thermo Scientific Co.).

2.5. Confocal microscopy of miRNA-1 molecular beacon

C2C12 cells (0.1×10^4) were seeded into 6-well plates containing cover glass. After 24 h, 50 pmole of miRNA-1 was transfected using LipofectAMINE (Invitrogen). After incubation for 3 h at 37 °C, growth medium was replaced by differentiation medium (DMEM, 1% FBS). Cells were collected at days 0, 2, 4, and 6 after induction of differentiation. After washing with Dulbecco's phosphate-buffered saline (D-PBS) twice for 15 min, cells were fixed with 500 μl of 3.7% formaldehyde for 15 min at 4 °C. After washing with D-PBS again, DAPI (4′,6-diamidino-2-phenylindole) staining (Vector Laboratories, CA) was performed, and confocal images were obtained (Carl Zeiss Inc., Germany).

2.6. Construction of CMV/Fluc and CMV/Gluc/3xPT_miRNA-1 vectors

A vector containing the firefly luciferase (Fluc) gene driven by a CMV promoter (designated as CMV/Fluc) was constructed. The Fluc reporter system was used to monitor the cellular homing and quantification of viable cells. We constructed the Gluc reporter system (CMV/Gluc/3xPT_miR-1) containing three copies of a perfect complementary miRNA-1 target sequence and fused it after the Gluc stop codon. The sequence of 3xPT_ miR-1 is: 5′ tcgagaatctagtATACATACTTCTTTACATTCCAtagta ATACATACTTCTTTACATTCCAtagtaATACATACTTCTTTACATTCCAt3′, 5′ ctagaTGGAA TGTAAAGAAGTATGTATtactaTGGAATGTAAAGAAGTATGTATtactaTGGAATGTAAAGAA GTATGTATAcTagattc 3′. The double-stranded oligonuleotide was subcloned into the Xho1 and Xba1 sites of CMV/Gluc to create CMV/Gluc/3xPT_miR-1. Three copies of perfect miRNA-1 targets before the poly (A) tail enhanced the response of CMV/Gluc to the repressive activity of miRNA-1.

As a negative control, CMV/Gluc/3xPT_miR-9 containing three copies of a perfect complementary miR-9 target sequence was constructed (25). The sequence of 3xPT_miR-9 is: 5′ tcgagaaTCTAGTTCATACAGCTAGATAACCAAAGAtagtaTCATA CAGCTAGATAACCAAAGA tagtaTCATACAGCTAGATAACCAAAGAt3′, 5′ctagaTCTTTG GTTATCTAGCTGTATGAtactaTCTTTGGTTATCTA GCTGTATGAtactaTCTTTGGTTATCTAG CTGTATGAactagattc 3′.

2.7. Luciferase assay for Fluc and Gluc activities

HeLa cells were seeded into 24-well plates at 5×10^4 cells per well. After 24 h incubation, transfection of the CMV/Fluc and CMV/Gluc/3xPT_miR-1 vectors was performed using LipofectAMINE Plus reagent (Invitrogen). CMV/Gluc/3xPT_miR-9 was transfected as a negative control. Target miRNA-1 was administered at concentrations of 0, 0.5, 1, 2.5, and 5 nmole. 4–8 h after transfection, cells were washed with phosphate-buffered saline (PBS) and treated with 100 μl of lysis solution. Supernatants were plated in microplates and Gluc and Fluc activities were measured using a Synergy MX (Bio-Tek, Ltd.) using a luciferase assay kit (TargetingSystems, USA). All results are displayed as means ± standard deviation (SD; $n = 4$).

Bioluminescence imaging obtained from an *ex vivo* specimen of a C2C12 cell-injected mouse was acquired by IVIS spectrum (Xenogen). Tissue samples from both thighs were sectioned 2 days after implantation and treated with 100 μl of lysis solution. Supernatants were plated in microplates and Gluc and Fluc activities were measured using a luciferase assay kit (TargetingSystems, USA).

Myogenic differentiation was induced in C2C12 cells as previously described (31). On days 0, 2, 4, and 6, C2C12 cells were seeded into 24-well plates at 5×10^4 cells per well. After 24 h incubation, cells were transfected with the CMV/Fluc and CMV/Gluc/3xPT_miR-1 vectors using LipofectAMINE Plus reagent (Invitrogen). Luciferase activity was measured in the C2C12 cells on days 0, 2, 4, and 6.

2.8. In vivo imaging of miRNA-1 by the dual optical miRNA-1 imaging systems

All *in vivo* experiments were housed under specific pathogen-free conditions and approved by institutional animal care and use committee in Yonsei University.

For *in vivo* imaging of miRNA-1 during myogenesis, CMV/Gluc/3xPT_miR-1 and miR-1 MB with an internal control, CMV/Fluc, were co-transfected into C2C12 cells. Myogenic differentiation was induced by changing the C2C12 medium (DMEM, 1% FBS). 1×10^7 of differentiated and undifferentiated C2C12 cells were injected subcutaneously into the right thigh and left thigh of nude mice (male BALB/c, 7 weeks old), respectively. The mice was scanned using IVIS spectrum (Xenogen, CA) ($n = 4$, mice). For the bioluminescence imaging of CMV/Gluc/3xPT_miR-1 and CMV/Fluc and fluorescence imaging of miR-1 MB, mice were anesthetized in an IVIS imaging chamber equipped with a small holder connected to an isoflurane and oxygen tank. Anesthetic gas was administered with 2% isoflurane in O_2 gas at a flow rate of 1 L min^{-1} through a nose cone. For bioluminescence imaging, 4 mg of D-luciferin for Fluc imaging and 100 μg of coelenterazine for Gluc imaging were intraperitoneally injected. The *in vivo* fluorescence imaging was conducted using a red filter (570–620 nm, band-pass filter; 600 nm, long-pass filter). A camera was used to acquire captured images at constant exposure times (1 s).

2.9. Histologic exam

Three days after injection of C2C12 cells, mice were sacrificed and implanted C2C12 tissue was isolated. C2C12 tissue was fixed in 4% paraformaldehyde and

embedded in paraffin. Histological sections were stained with hematoxylin and eosin for microscopic evaluation. Immunohistochemical analysis was performed with myogenin antibody.

3. Results

3.1. Design of the dual optical miRNA-1 imaging systems

To image miRNA-1 biogenesis during myogenesis by the dual optical imaging systems, we designed both a Gluc reporter gene-based signal-off system and MB-based signal-on imaging system. The miRNA-1 reporter gene was designed to have perfectly targeted binding sequences against miRNA-1 by cloning three copies of reverse complimentary oligonucleotide sequences (3xPT_miR-1) to mature miRNA-1 into the 3′ UTR of the Gluc reporter gene (designated as CMV/Gluc/3xPT_miR-1; Fig. 1A). In the absence of miRNA-1, the luciferase signal of CMV/Gluc/3xPT_miR-1 turns on, and in the presence of miRNA-1, it is off by the function of miRNA-1. The miR-1 MB was designed to form a stem-loop structure with a copy of the complementary sequences to mature miRNA-1, labeled with Texas Red-X (absorbance/emission wavelength: 590/615 nm) as a fluorescent signal and BHQ2 as a quenching molecule at each end (designated as miR-1 MB; Fig. 1B). When miRNA-1 is present and binds to the complementary sequences within miR-1 MB, a conformational change occurs in the MB producing a fluorescent signal.

3.2. Specificity of miRNA-1 reporter gene and miR-1 MB

To demonstrate the specificity of the dual optical miRNA-1 imaging systems, we first investigated the expression of miRNA-1 in various cell lines C2C12, H9C2 (cardiac myoblast cells), HT-ori3 (normal thyroid cells), ARO (thyroid carcinoma cells), C6 (glioma cells), and HeLa (cervical cancer cells) cells by real-time PCR using specific primers for mature miRNA-1. Similar to other reports, C2C12 and H9C2 cells showed relatively high expression of miRNA-1(32, 33) while HT-ori3, ARO, C6, and HeLa cells showed little or no expression of miRNA-1 (Suppl. Fig. 1). To determine the signal-off specificity of the miRNA-1 reporter gene, CMV/Gluc/3xPT_miR-1 was transfected into HeLa cells, which do not express miRNA-1. Exogenously introduced miRNA-1 in HeLa cells resulted in a dramatic bioluminescence decrease from CMV/Gluc/3xPT_miR-1 with 2.5 and 5 nmole of miRNA-1 (Fig. 2A). On the other hand, CMV/Gluc/3xPT_miR-9, reported previously as a signal-off imaging system to detect miRNA-9 (25), was transfected into HeLa cells and showed no significant repression of bioluminescence signal in response to exogenous miRNA-1. To test the signal-on specificity of the miR-1 MB, HeLa cells were selected as a negative cell line for expression of miRNA-1. In the absence of exogeneous miRNA-1, the fluorescence signals from the miR-1 MB transfected into HeLa cells remained quenched (Fig. 2B). However, when various amounts of exogeneously synthesized miRNA-1 were co-transfected into HeLa cells, the miR-1 MB showed a dose-dependent and gradual increase in fluorescence activity. The maximal fluorescence intensity of the miR-1 MB was 3-fold higher than that of the quenched state in response to miRNA-1. Importantly, the miR-1 MB remained quenched after administration of a high dose of miRNA-9 as a control. Fluorescence activity of miR-1 MB was stably quenched in HeLa cells for 2 days in the absence of exogeneous miRNA-1 (Suppl. Fig. 2). After co-transfection of 0.5 nmole exogeneous miRNA-1 with miR-1 MB into HeLa cells, the fluorescence signals were restored due to the hybridization of miRNA-1 with miR-1 MB, leading to the unquenching of the miR-1 MB. These findings demonstrate that both CMV/Gluc/3xPT_miR-1 and miR-1 MB have specificity in detecting miRNA-1 as a signal-off and a signal-on imaging system, respectively.

3.3. Decrease in bioluminescence signals of CMV/Gluc/3xPT_miR-1 and increase in fluorescence activities of miR-1 MB during myogenesis

To monitor miRNA-1 by CMV/Gluc/3xPT_miR-1 or miR-1 MB during myogenesis, C2C12 cells were induced into skeletal

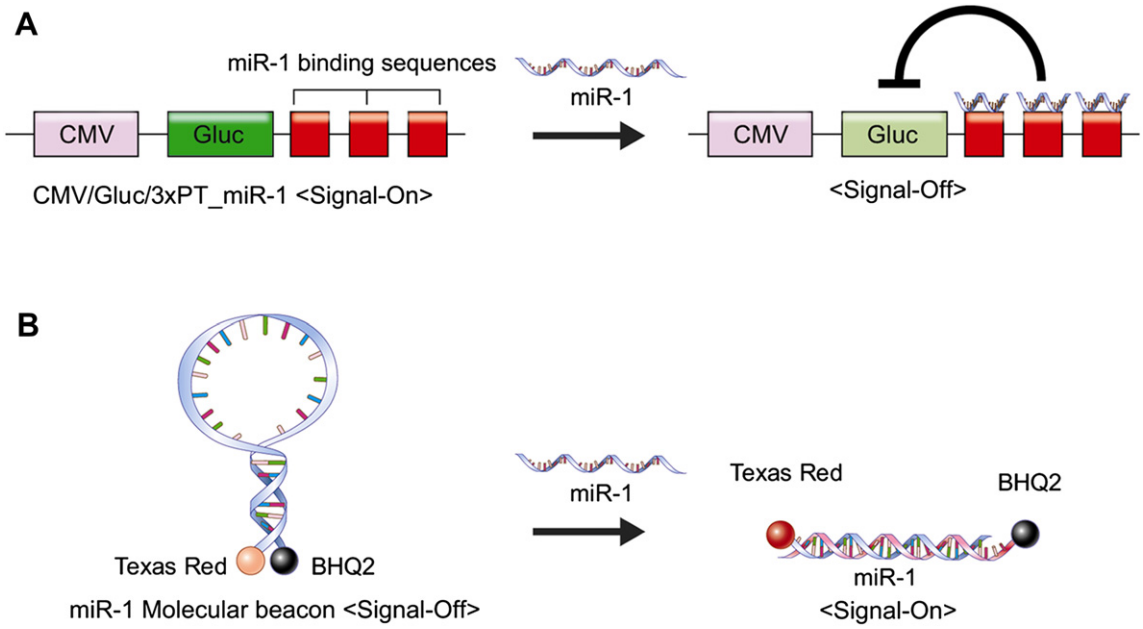

Fig. 1. A schematic illustration of a dual optical miRNA imaging systems to monitor miRNA-1 expression. (A) CMV/Gluc/3xPT_miR-1 constructs. Gluc regulated by CMV promoter carries three copies of the target sequence complementary to miRNA-1 in its 3′ UTR. In the absence of miRNA-1, Gluc activity regulated CMV promoter is always on, but in the presence of miRNA-1, hybridization of miRNA-1 with CMV/Gluc/3xPT_miR-1 results in miRNA-1-regulating repression of Gluc signals. (B) MiR-1 MB was designed to have Texas Red-X as a fluorophore and BHQ2 as a quencher (absorbance/emission wavelength: 590/615 nm). The MB forms a stem-loop structure keeping the fluorophore and quencher in close proximity. With the stem-loop structure is preserved, fluorescence signal from the fluorophore is absorbed into the nearby quencher by FRET. When target miRNA-1 binds to the complementary sequences within the MB, double strand hybridization occurs, producing fluorescence signal.

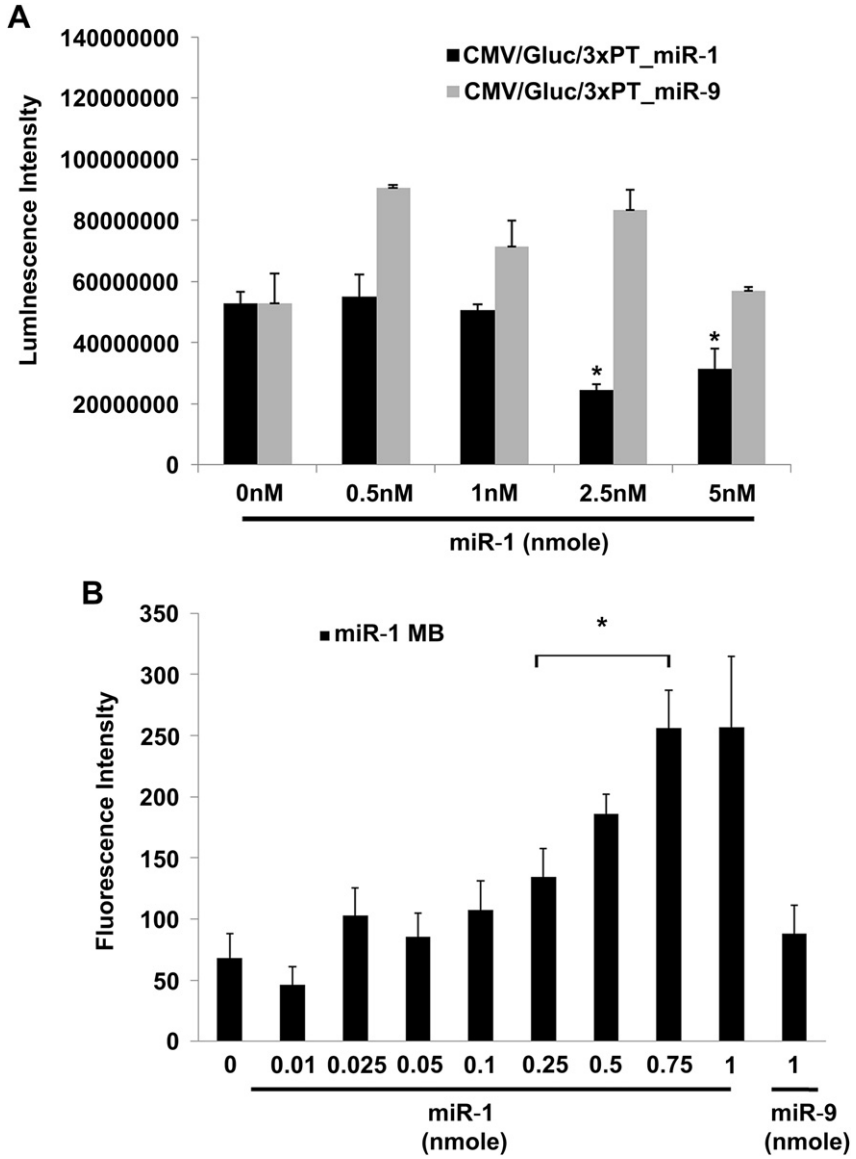

Fig. 2. Confirmation of specific binding of CMV/Gluc/3xPT_miR-1 and miR-1 MB to miRNA-1 in HeLa cells. (A) Luminescence intensity of CMV/Gluc/3xP_miR-1 and a negative control, CMV/Gluc/3xPT_miR-9, transfected into HeLa cells. After administration of miRNA-1, luminescence intensity of CMV/Gluc/3xPT_miR-1 shows a significant decrease at a dose of 2.5 nmole of miRNA-1, while no significant decrease of luminescence was detected in CMV/Gluc/3xPT_miR-9. Data are displayed as mean ± standard error (*$P < 0.005$). (B) Fluorescence analysis of miR-1 MB in HeLa cells. Fluorescence intensity increases with the dose of miRNA-1 administered for up to 1 nmole. Data are displayed as mean ± standard error (*$P < 0.005$). After administration of 1 nmole of miRNA-9 to miR-1 MB in HeLa cells, there was no significant increase of fluorescence intensity.

myogenic differentiation by withdrawing serum from the culture medium. RT-PCR for one of the myogenic markers, myogenin, showed a gradual increase in mRNA during myogenesis, demonstrating successful skeletal muscle differentiation (Suppl. Fig. 3). Quantitative real-time PCR analysis revealed a gradual increase in miRNA-1 expression during skeletal muscle differentiation in C2C12 cells (Fig. 3A). To image the gradual expression of endogenous miRNA-1 during myogenesis by the signal-off miRNA-1 imaging system, the CMV/Gluc/3xPT_miR-1 vector was transfected into C2C12 cells and further induced into myogenic differentiation. Gluc activity, representing endogenous miRNA-1 expression, was significantly and gradually decreased during myogenesis, as observed for the gradual increase in endogenous level of miRNA-1 after skeletal muscle differentiation by real-time PCR (Fig. 3B). Similarly, to show the gradual increase in miRNA-1 during myogenesis by the signal-on miRNA-1 imaging system, miR-1 MB was transfected into both undifferentiated and differentiated C2C12 cells. After induction of differentiation of the cells, the gradual increase in fluorescence signal from the miR-1 MB was observed, which represented intrinsic miRNA-1 expression during myogenesis (Fig. 3C). An approximate 5.3-fold increase in the fluorescence signal of miR-1 MB was noted 6 days after skeletal muscle differentiation. Increased fluorescence signal during myogenesis was expected due to separation of the fluorophore and quencher after hybridization between the miRNA-1 and miRNA binding sequences. To obtain signal-on fluorescence images of the intracellularly and gradually expressed miRNA-1 from a single cell during myogenesis of C2C12 cells, confocal microscopic analysis was conducted on either a single undifferentiated or differentiated C2C12 cell transfected with the miR-1 MB. Similar to the quantitative fluorescence analysis of the miR-1 MB during myogenesis in Fig. 3C, fluorescence brightness in the cytoplasm of a single C2C12 cell gradually increased for up to 6 days after induction of differentiation due to the gradual increase in miRNA-1 expression during

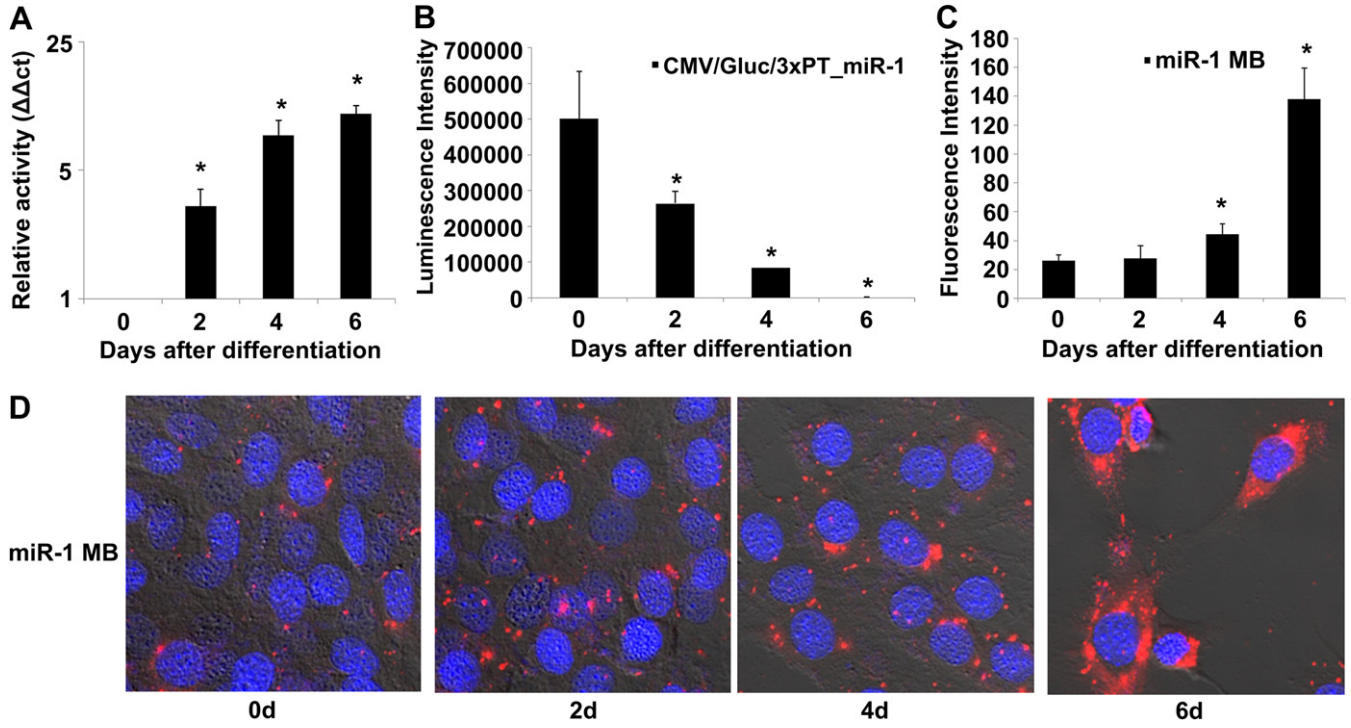

Fig. 3. *In vitro* imaging of miRNA-1 expression in C2C12 cells by individual application of CMV/Gluc/3xPT_miR-1 or miR-1 MB. (A) Real-time qRT-PCR using miRNA-1 primer in C2C12 cells after induction of differentiation induction. MiRNA-1 expression level shows gradual increase after differentiation induction up to 6 days. Data are displayed as mean ± standard error of relative activity ($^*P < 0.05$). (B) Luminescence intensity of CMV/Gluc/3xPT_miR-1 in C2C12 cells after induction of differentiation. Luminescence signal from CMV/Gluc/3xPT_miR-1 shows a pattern of gradual decrease from D2 to D6 after differentiation induction. Data are displayed as mean ± standard error ($^*P < 0.005$). (C) Fluorescence intensity of miR-1 MB in C2C12 cells after induction of myogenic differentiation. A gradual increase of fluorescence signal is noted according to differentiation days. Data are displayed as mean ± standard error ($^*P < 0.005$). (D) Confocal microscopy imaging (×800) of C2C12 cells transfected with miR-1 MB. After induction of differentiation, confocal microscopy image was obtained up to 6 days. Excitation and emission wavelength for Texas Red-X were 590 nm and 615 nm, respectively. All images were merged with the DAPI image (nucleus staining, 460 nm) and cellular morphology. Confocal microscopy images show gradual increasing fluorescence signal-on cytoplasm of C2C12 cells according to differentiation days.

myogenesis (Fig. 3D). Confocal microscopic images at day 6 revealed intense fluorescence signals in the entire cytoplasm of a single C2C12 cell, representing high expression of intrinsic miRNA-1 within the cytoplasm of differentiated mature C2C12 cells.

3.4. Simultaneous in vitro and in vivo imaging of a bioluminescent miRNA-1 reporter gene and the fluorescent miR-1 MB in a single C2C12 cell during myogenesis

To image miRNA-1 in a single C2C12 by the bioluminescent signal-off imaging system and the fluorescent signal-on imaging system simultaneously, CMV/Gluc/3xPT_miR-1 and the miR-1 MB were co-transfected into C2C12 cells, which were further induced into myogenic differentiation. Both bioluminescent and fluorescent imaging systems in a single C2C12 cell simultaneously showed a gradual difference in the signals of each imaging modality over several days of myogenic differentiation (Fig. 4A). Because a gradual increase in the endogneous level of miRNA-1 was observed during myogenesis of C2C12 cells, during 6 days of myogenic differentiation of these cells, the bioluminescence signals of CMV/Gluc/3xPT_miR-1 were significantly and gradually turned off, while the fluorescence signals of miR-1 MB were progressively turned on. But, in response of miRNA-1, the degree of decreased luciferase signals was much higher than that of increases fluorescence signals due to the difference in sensitivity of each imaging modality. Similar with the results of Fig. 3D, gradual fluorescence brightness of miR-1 MB in the cytoplasm of C2C12 cells during myogenesis was observed from the co-transfection of CMV/Gluc/3xPT_miR-1 and the miR-1 MB (Fig. 4B).

For *in vivo* imaging of miRNA-1 by the dual optical imaging systems, CMV/Gluc/3xPT_miR-1 and the miR-1 MB were transfected into 1×10^7 C2C12 cells and then injected subcutaneously into both thighs of a nude mouse. As an internal control, plasmid CMV/Fluc, where Fluc expression is constant regardless of miRNA-1 expression or myogenic differentiation, was co-transfected into C2C12 cells with the dual optical miRNA imaging systems. Only C2C12 cells xenografted into the right thigh were induced to undergo myogenic differentiation. The Fluc signals were not significantly different between cells without differentiation induction in the left thigh and cells with differentiation induction in the right thigh for 2 days, which demonstrated that the numbers of surviving cells were equal in both thighs (Fig. 4C, lower). However, from the same mouse, the dual optical miRNA-1 imaging systems in the right thigh showed a gradual difference in both bioluminescence and fluorescence signals for 2 days due to the myogenic differentiation-dependent gradual increase in miRNA-1 expression. The bioluminescence signals of CMV/Gluc/3xPT_miR-1 from the differentiated cells in the right thigh were significantly lower than those from the undifferentiated cells in the left thigh (Fig. 4C, upper). In contrast, the fluorescence signals from the miR-1 MB in the right thigh were significantly higher than those in the left thigh (Fig. 4C, middle). Fold changes of CMV/Gluc/3xPT_miR-1 and miR-1 MB signals, as determined by region of interest (ROI) on undifferentiated cells in the left thigh and differentiated cells in the right thigh, showed 4- and 20-fold lower bioluminescence and 3- and 12-fold higher fluorescence signals at day 1 and day 2, respectively (Suppl. Fig. 4A).

To verify *in vivo* optical signals of the dual optical miRNA-1 imaging systems during myogenesis, the implanted C2C12 cells in

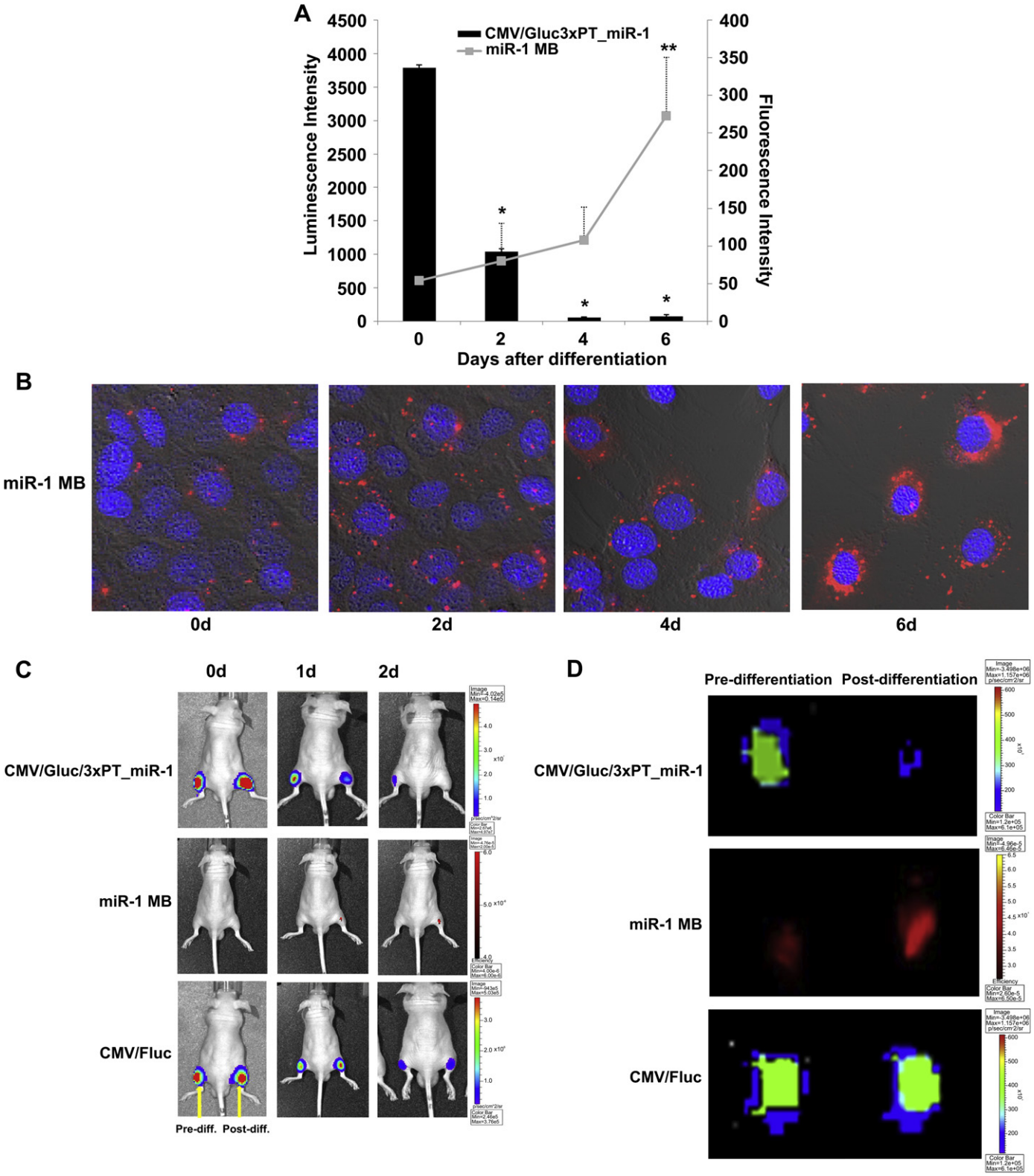

Fig. 4. Bioimaging of miRNA-1 expression in a single C2C12 cell by the dual optical miRNA-1 imaging systems. A single C2C12 cell was co-transfected with miR-1 MB and CMV/Gluc/3xPT_miR-1 and further induced into myogenic differentiation. *In vitro* data was acquired for 6 days and *in vivo* for 2 days. (A) Comparison of longitudinal changes in fluorescence signal from miRNA-1 beacon and luminescence signal from CMV/Gluc/3xPT_miR-1 in C2C12 cells after induction of differentiation. Data are displayed as mean ± standard error ($^{*}P < 0.005$, $^{**}P < 0.01$). (B) Confocal microscopy imaging (×800) of miR-1 MB obtained from a dual optical miRNA-1-transfected single C2C12 cell. (C) *In vivo* imaging of miRNA-1 by the dual optical miRNA-1 imaging systems during myogenesis of C2C12 cells. CMV/Gluc/3xPT_miR-1 and miR-1 MB with an internal control, CMV/Fluc, were co-transfected into C2C12 cells. A nude mouse injected with differentiated C2C12 cells in the right thigh and undifferentiated C2C12 cells in the left thigh. Gluc signal from CMV/Gluc/3xPT_miR-1 shows a rapid decrease from right thigh, suggesting signal decrease caused by induction of differentiation (upper row). Simultaneously, fluorescence signal from the miR-1 MB shows a progressive increase from the right thigh, representing higher expression of miRNA-1 on differentiated cells during myogenesis (lower row). Meanwhile, Fluc signal from CMV/Fluc shows the same pattern from both thighs indicating similar cellular survival for up to 2 days between differentiated cells and undifferentiated cells (middle row). (D) *Ex vivo* confirmation of *in vivo* imaging signals by the dual optical miRNA-1 imaging systems during myogenesis. Tissue samples from both thighs were sectioned 2 days after implantation of C2C12 cells, and fluorescence imaging for miR-1 MB was obtained (Ex: 590 nm, Em: 615 nm). Fluorescence signal from the differentiated specimen (right thigh) is higher than that from the undifferentiated specimen (left thigh) (middle row). Bioluminescence from CMV/Gluc/3xPT_miR-1 showed a decreased intensity after differentiation (upper row) while that from CMV/Fluc had no clear difference between pre-differentiation and post-differentiation.

both thighs were obtained 2 days after myogenic differentiation. The optical imaging analysis showed that the decrease in bioluminescent signals from CMV/Gluc/3xPT_miR-1 and increase in fluorescent signals from the miR-1 MB from sampled tissues of the right thigh were much greater than those obtained from the left thigh (Fig. 4D, upper and middle). However, the bioluminescent imaging of CMV/Fluc did not show a significant difference between sampled tissues of the left and right thigh (Fig. 4D, lower). Immunohistochemical analysis using myogenin antibody verified that myogenic differentiation had progressed in tissue from the right thigh, while myogenin expression was minimal in tissue sampled from the left thigh (Suppl. Fig. 4B). Confocal microscopy of sectioned slides from tissue samples of both thighs showed higher fluorescence signals in the cytoplasm of differentiated C2C12 cells than that of undifferentiated C2C12 cells (Suppl. Fig. 4C). These results verified that the decrease in the bioluminescent signals of CMV/Gluc/3xPT_miR-1 and the increase in fluorescent signals of miR-1 MB were due to the myogenic differentiation-dependent increase in the endogeneous level of miRNA-1.

4. Discussion

The assessment of miRNA expression specific to tissues or diseases is very important in providing meaningful information about miRNA function in cellular development and disease. However, most methods of detecting miRNA expression including microarray, Northern blot and real-time PCR are time consuming and laborious and, additionally, require the sacrifice of animals to analyze miRNA biogenesis. Our miRNA imaging system using a reporter gene and the MB have successfully allowed us to repeatedly monitor miRNA biogenesis during neurogenesis, myogenesis, and carcinogenesis *in vitro* and *in vivo* (24–31) in a noninvasive manner. To date, individual application of the reporter gene- or MB-based miRNA imaging system has been studied, but has not been fully competent for visualization of miRNA biogenesis *in vitro* and *in vivo* due to the limitations of each imaging system. Although bioluminescence imaging of the miRNA reporter gene provides good imaging sensitivity for the detection of miRNA biogenesis, as a signal-off system it is difficult to distinguish between decreased bioluminescence signals due to miRNA-altered gene expression or cellular loss. On the other hand, fluorescence imaging provides a signal-on imaging system that indicates miRNA expression. However, due to high autofluorescence backgrounds, the miRNA MB is frequently challenged to obtain high quality *in vivo* images. In this study, simultaneous *in vitro* and *in vivo* bioluminescence and fluorescence imaging of the miRNA-1 reporter gene and the miR-1 MB successfully visualized miRNA-1 biogenesis during myogenesis of C2C12 cells by providing complementary information to overcome the shortcomings of each miRNA imaging system. Although the *in vitro* and *in vivo* bioluminescent signals by the miRNA-1 reporter gene were undetectable at the end of the myogenic differentiation period tested, compared to undifferentiated C2C12 cells the additional *in vitro* and *in vivo* fluorescent signals by the miR-1 MB from the same subject successfully provided complementary evidence of the increase in miRNA-1 during myogenesis. This result implies that the decrease in bioluminescent signals was caused by the increase in miRNA-1 expression during myogenesis. Additionally, the *in vitro* miRNA-1 expression pattern during myognesis, represented by the gradual decrease in bioluminescent signal of the miRNA-1 reporter gene, was easily visualized in a single C2C12 cell by confocal microscopy analysis of miR-1 MB. However, there might be one question that the dual optical miRNA-1 imaging system can block miRNA-1 function because the successful imaging of each miRNA-1 biosensor was resulted in the hybridization of miRNA-1 expressed in the differentiated C2C12 cells. Kim *et al* [32] demonstrated that miR-221 MB transfected more than 300 pmol into cells significantly affected on miRNA-221 function but less than 200 pmol did not significantly affect on miRNA-221 function. From the results of *in vivo* imaging (Fig. 4C) and *ex vivo* confirmation (Suppl. Fig. 4B and C), co-transfection of 50 pmol of miRNA-1 molecular beacon and CMV/Gluc/3xPT_miR-1 into C2C12 cells did not block the expression of miRNA-1 and myogenic differentiation indicating no significant affect on miRNA-1 function. This is the first report of imaging a miRNA using a miRNA reporter gene and the miRNA MB simultaneously. The results of this study demonstrate that the dual optical miRNA-1 imaging systems could provide more accurate imaging information about miRNA-1 biogenesis than the individual application of each miRNA imaging system.

MiRNA-1 is highly expressed in cardiac and skeletal myocytes, and is associated with the myogenic differentiation process; miRNA-1 has been reported to be associated with cardiac muscular disease such as cardiomyopathy [33,34]. The evaluation of miRNA-1 expression and its control is of great value in understanding the mechanism of disease and developing treatment methods. MiRNAs, including miRNA-1, miRNA-206, miRNA-26a, and miRNA-133 are associated with myogenic differentiation and disease progression [35–37]. Therefore, a dual optical miRNA imaging systems for monitoring miRNA expression associated with disease processes will be useful in the early detection of disease and in the understanding of biologic processes during pathogenesis. In particular, the *in vivo* dual optical miRNA imaging systems can allow noninvasive real-time visualization, with the ease of longitudinal studies.

5. Conclusion

We developed a dual optical miRNA-1 imaging systems to monitor miRNA-1 expression in a single cell using the miRNA-1 reporter gene and a miR-1 MB. Both imaging systems have unique advantages, and their roles in visualizing miRNA expression are complementary. The dual optical miRNA-1 imaging systems, which was used to successfully monitor miRNA-1 biogenesis during myogenesis *in vitro* and *in vivo*, can be applied to animal models associated with miRNA-related disease to obtain more information on disease progression.

Acknowledgements

This work was supported by Nuclear Research & Development Program of National Research Foundation of Korea (NRF) funded by the Ministry of Education, Science & Technology (MEST) (grant code: 2010-0018684) and the Bio & Medical Technology Development Program of the National Research Foundation (NRF) funded by the Korean government (MEST) (No. 2012-0006097). The authors are grateful to Dong-Su Jang for the illustration

Appendix A. Supplementary data

Supplementary data associated with this article can be found, in the online version, at doi:10.1016/j.biomaterials.2012.05.056.

References

[1] Lee RC, Feinbaum RL, Ambros V. The *C. elegans* heterochronic gene lin-4 encodes small RNAs with antisense complementarity to lin-14. Cell 1993; 75:843–54.
[2] Zamore PD, Haley B. Ribo-gnome: the big world of small RNAs. Science 2005; 309:1519–24.
[3] Sullivan CS, Ganem D. MicroRNAs and viral infection. Mol Cell 2005;20:3–7.
[4] Croce CM, Calin GA. miRNAs, cancer, and stem cell division. Cell 2005;122: 6–7.

[5] Iorio MV, Croce CM. MicroRNAs in cancer: small molecules with a huge impact. J Clin Oncol 2009;27:5848–56.
[6] Zeng Y, Yi R, Cullen BR. MicroRNAs and small interfering RNAs can inhibit mRNA expression by similar mechanisms. Proc Natl Acad Sci U S A 2003;100:9779–84.
[7] Navarro L, Dunoyer P, Jay F, Arnold B, Dharmasiri N, Estelle M, et al. A plant miRNA contributes to antibacterial resistance by repressing auxin signaling. Science 2006;312:436–9.
[8] Lagos-Quintana M, Rauhut R, Yalcin A, Meyer J, Lendeckel W, Tuschl T. Identification of tissue-specific microRNAs from mouse. Curr Biol 2002;12:735–9.
[9] Callis TE, Wang DZ. Taking microRNAs to heart. Trends Mol Med 2008;14:254–60.
[10] Callis TE, Chen JF, Wang DZ. MicroRNAs in skeletal and cardiac muscle development. DNA Cell Biol 2007;26:219–25.
[11] Thum T, Catalucci D, Bauersachs J. MicroRNAs: novel regulators in cardiac development and disease. Cardiovasc Res 2008;79:562–70.
[12] Kim HK, Lee YS, Sivaprasad U, Malhotra A, Dutta A. Muscle-specific microRNA miR-206 promotes muscle differentiation. J Cell Biol 2006;174:677–87.
[13] Wong CF, Tellam RL. MicroRNA-26a targets the histone methyltransferase enhancer of zeste homolog 2 during myogenesis. J Biol Chem 2008;283:9836–43.
[14] Chen JF, Mandel EM, Thomson JM, Wu Q, Callis TE, Hammond SM, et al. The role of microRNA-1 and microRNA-133 in skeletal muscle proliferation and differentiation. Nat Genet 2006;38:228–33.
[15] Chen JF, Tao Y, Li J, Deng Z, Yan Z, Xiao X, et al. microRNA-1 and microRNA-206 regulate skeletal muscle satellite cell proliferation and differentiation by repressing Pax7. J Cell Biol 2010;190:867–79.
[16] Elia L, Contu R, Quintavalle M, Varrone F, Chimenti C, Russo MA, et al. Reciprocal regulation of microRNA-1 and insulin-like growth factor-1 signal transduction cascade in cardiac and skeletal muscle in physiological and pathological conditions. Circulation 2009;120:2377–85.
[17] Zhao Y, Samal E, Srivastava D. Serum response factor regulates a muscle-specific microRNA that targets Hand2 during cardiogenesis. Nature 2005;436:214–20.
[18] Miska EA, Alvarez-Saavedra E, Townsend M, Yoshii A, Sestan N, Rakic P, et al. Microarray analysis of microRNA expression in the developing mammalian brain. Genome Biol 2004;5:R68.
[19] Thomson JM, Parker J, Perou CM, Hammond SM. A custom microarray platform for analysis of microRNA gene expression. Nat Methods 2004;1:47–53.
[20] Li W, Ruan K. MicroRNA detection by microarray. Anal Bioanal Chem 2009;394:1117–24.
[21] Varallyay E, Burgyan J, Havelda Z. MicroRNA detection by northern blotting using locked nucleic acid probes. Nat Protoc 2008;3:190–6.
[22] Varkonyi-Gasic E, Wu R, Wood M, Walton EF, Hellens RP. Protocol: a highly sensitive RT-PCR method for detection and quantification of microRNAs. Plant Methods 2007;3:12.
[23] Chen C, Ridzon DA, Broomer AJ, Zhou Z, Lee DH, Nguyen JT, et al. Real-time quantification of microRNAs by stem-loop RT-PCR. Nucleic Acids Res 2005;33:e179.
[24] Lee JY, Kim S, Hwang do W, Jeong JM, Chung JK, Lee MC, et al. Development of a dual-luciferase reporter system for in vivo visualization of microRNA biogenesis and posttranscriptional regulation. J Nucl Med 2008;49:285–94.
[25] Ko MH, Kim S, Hwang do W, Ko HY, Kim YH, Lee DS. Bioimaging of the unbalanced expression of microRNA9 and microRNA9* during the neuronal differentiation of P19 cells. FEBS J 2008;275:2605–16.
[26] Kim HJ, Kim YH, Lee DS, Chung JK, Kim S. In vivo imaging of functional targeting of miR-221 in papillary thyroid carcinoma. J Nucl Med 2008;49:1686–93.
[27] Kim HJ, Chung JK, Hwang do W, Lee DS, Kim S. In vivo imaging of miR-221 biogenesis in papillary thyroid carcinoma. Mol Imaging Biol 2009;11:71–8.
[28] Ko HY, Lee DS, Kim S. Noninvasive imaging of microRNA124a-mediated repression of the chromosome 14 ORF 24 gene during neurogenesis. FEBS J 2009;276:4854–65.
[29] Ko HY, Hwang do W, Lee DS, Kim S. A reporter gene imaging system for monitoring microRNA biogenesis. Nat Protoc 2009;4:1663–9.
[30] Hwang do W, Song IC, Lee DS, Kim S. Smart magnetic fluorescent nanoparticle imaging probes to monitor microRNAs. Small 2010;6:81–8.
[31] Kang WJ, Cho YL, Chae JR, Lee JD, Choi KJ, Kim S. Molecular beacon-based bioimaging of multiple microRNAs during myogenesis. Biomaterials 2011;32:1915–22.
[32] Kim JK, Choi KJ, Lee M, Jo MH, Kim S. Molecular imaging of a cancer-targeting theragnostics probe using a nucleolin aptamer- and microRNA-221 molecular beacon-conjugated nanoparticle. Biomaterials 2012;33:207–17.
[33] Sayed D, Hong C, Chen IY, Lypowy J, Abdellatif M. MicroRNAs play an essential role in the development of cardiac hypertrophy. Circ Res 2007;100:416–24.
[34] Ikeda S, He A, Kong SW, Lu J, Bejar R, Bodyak N, et al. MicroRNA-1 negatively regulates expression of the hypertrophy-associated calmodulin and Mef2a genes. Mol Cell Biol 2009;29:2193–204.
[35] Xiao J, Luo X, Lin H, Zhang Y, Lu Y, Wang N, et al. MicroRNA miR-133 represses HERG K+ channel expression contributing to QT prolongation in diabetic hearts. J Biol Chem 2007;282:12363–7.
[36] Yang B, Lin H, Xiao J, Lu Y, Luo X, Li B, et al. The muscle-specific microRNA miR-1 regulates cardiac arrhythmogenic potential by targeting GJA1 and KCNJ2. Nat Med 2007;13:486–91.
[37] Care A, Catalucci D, Felicetti F, Bonci D, Addario A, Gallo P, et al. MicroRNA-133 controls cardiac hypertrophy. Nat Med 2007;13:613–8.